Effect of Silica as Fillers on Polymer Interdiffusion in Poly(butyl methacrylate) Latex Films

Mitsuru Kobayashi,† Yahya Rharbi, Laurent Brauge, Lan Cao, and Mitchell A. Winnik*

Department of Chemistry, University of Toronto, 80 St. George Street, Toronto, ON, M5S 3H6, Canada

Received September 10, 2001; Revised Manuscript Received June 11, 2002

ABSTRACT: In this paper, we examine the influence of silica as fillers on polymer interdiffusion in poly(butyl methacrylate) latex films. We carry out fluorescence resonance energy transfer (FRET) measurements on latex films that allow us to follow the extent of polymer diffusion as a function of time after the latex/pigment dispersion dries. In this study, we compare four different types of colloidal silica and discuss how fillers affect the rate of polymer interdiffusion in latex films. The efficiency of energy transfer data for newly formed films indicate that 54 and 73 nm diameter SiO_2 particles have little or no effect on the interfacial area between donor- and acceptor-labeled latex cells, whereas the 16 and 27 nm SiO_2 particles significantly reduce the interfacial area with increasing amounts of filler. The maximum efficiency of energy transfer data indicate that 16 and 27 nm SiO_2 also affect the extent of mixing that can be achieved in 200 h annealing at 60 °C. The rate of polymer interdiffusion in latex films is retarded as one increases the amount of filler, and this rate decreases as the filler size decreases. Our results can be explained with a free volume model that assumes that the surface of the silica particles raises the effective glass transition temperature of the matrix.

Introduction

Many polymer coatings used in a wide variety of applications such as paints and paper coatings, contain a large amount of inorganic/organic pigments. One of the major reasons for introducing these pigments is that hard fillers can reinforce soft polymeric matrices. For example, natural or synthetic rubber is commonly reinforced by carbon black particles, and silicone elastomers (PDMS) can be reinforced by silica.[1] Since silica is chemically inactive and optically transparent, it can be used in a wide range of applications, ranging from paints and magnetic fluids to high-quality paper coatings.[2] In the paints and adhesives industries, vinyl acetate, acrylic ester, synthetic rubber, and other polymer latexes have been used in coatings and adhesives for fabric and paper.[3] Colloidal silica is used with these polymer emulsions in order to improve adhesion, durability, and abrasion resistance. The silica also serves to prevent stickiness and improves the washing resistance of the coatings. When colloidal silica is used as a constituent for paints, a superior stain resistant film can be formed due to its antistatic characteristics. In paper coatings, this property provides better quality on sheet feeding, and thus silica is used as an antistatic agent.

Colloidal silica is also widely used for paper coatings. For instance, high-quality coated paper for graphics printing has a smooth layer on the top of the coating in order to enhance gloss.[4] Other inorganic pigments, such as clay, calcium carbonate, talc, alumina, and titanium dioxide, are also used with latex polymers to avoid stickiness to the stainless steel drum. For this type of paper, one would like to make the surface of the paper more rigid, in other words, to prevent it from sticking to the hot stainless steel drum.

Another application of (colloidal) silica for high-quality paper coatings is for photographic quality ink jet printing paper.[5] In this case, the coating contains both silica and a latex polymer with a relatively high glass transition temperature (T_g), as well as water-soluble polymers such as poly(vinyl alcohol), casein, and starch. The ink receiving layer is required to have a large pore volume to keep the ink jet printing ink at the surface of the coated paper, and dry the ink dispersion as quickly as possible. Silica also serves to prevent the ink dispersion from spreading horizontally and penetrating vertically. In this application, the latex particles act as silica binder, but are also required to keep their shape, which means that less coalescence is preferred in this system. These different applications of silica-plus-latex in coatings require a broad understanding of the nature of their interaction.

In this paper, we examine the influence of silica nanospheres on polymer interdiffusion in poly(butyl methacrylate) (PBMA) latex films. We carry out fluorescence resonance energy transfer (FRET) measurements on latex films that allow us to follow the extent of polymer diffusion as a function of time after the latex/pigment dispersion dries. In this study, we compare four different types of colloidal silica, and discuss how silica fillers affect the rate of polymer interdiffusion in latex films. We focus on the effect of silica particle size on polymer interdiffusion rate in poly(butyl methacrylate) latex films.

Experimental Section

Latex Samples. Butyl methacrylate (BMA) was distilled under vacuum prior to use. Potassium persulfate (KPS), sodium bicarbonate ($NaHCO_3$), sodium dodecyl sulfate (SDS), and 1-dodecanethiol were used as supplied. Distilled water was further purified through a Millipore Milli-Q system. Poly(butyl methacrylate) (PBMA) latex samples, labeled with 1 mol % of a fluorescent dye [either a donor, phenanthrene (Phe) or an

* To whom correspondence should be addressed. E-mail: mwinnik@chem.utoronto.ca.

† Permanent address: Imaging Media Development Laboratory, Oji Paper Co., Ltd., 1-10-6, Shinonome, Koto-ku, Tokyo, 135-8558, Japan.

10.1021/ma0115951 CCC: $22.00
Published on Web 08/08/2002

Table 1. Recipe for Preparing 100 nm PBMA Latex

	first stage (batch process)	second stage (under monomer-starved conditions)	
		Phe-labeled	An-labeled
BMA (g)	3.5	35.0	35.0
An-MA (g)			0.65[a]
Phe-MMA (g)		0.68[a]	
water (g)	57.0	27.0	27.0
KPS (g)	0.06	0.06	0.06
SDS (g)	0.21	0.60	0.60
$NaHCO_3$ (g)	0.08		
1-dodecanethiol (g)		0.30	0.30
T_{React}[b] (°C)	80	80	80
t_{React}[c] (h)	1.5	18	18

[a] 1 mol % relative to the total monomer fed in the second stage. [b] Reaction temperature. [c] Reaction time.

acceptor, anthracene (An)], were prepared by semicontinuous emulsion copolymerization at 80 °C, using KPS as the initiator, SDS as the surfactant, and 1-dodecanethiol as the chain transfer agent. The reaction conditions were similar to those described previously.[6] As a donor-labeled monomer, we used (9-phenanthryl)methyl methacrylate (Phe-MMA) to introduce the donor dye. As an acceptor-labeled monomer, we used 9-anthryl methacrylate (An-MA). The synthesis and characterization of these monomers have been described previously.[7]

The recipe for preparing 100 nm diameter PBMA latex particles is shown in Table 1. We used the same seed latex particles obtained in the first stage for preparing both the Phe- and An-labeled latex particles. The particle size and size distributions were determined by dynamic light scattering employing a Brookhaven BI-90 particle sizer. Molecular weight and molecular weight distributions were measured by gel permeation chromatography (GPC), using two Ultrastyragel columns (500 + 10^4 Å) with tetrahydrofuran (THF) as the eluent and a flow rate of 0.4 mL/min. These polymers were calibrated based upon poly(methyl methacrylate) (PMMA) standards. Dual detectors (refractive index and fluorescence detectors) were used to detect the presence of the donor and acceptor dyes and to ensure that these fluorescent dyes are randomly distributed in the polymer backbone. The glass transition temperatures (T_g) of the polymers were obtained elsewhere.[8] Their characteristics are shown in Table 2. These latex particles, referred to as PBMA, have a diameter of 100 nm and a T_g of 20 °C. The solid content of the dispersion was measured gravimetrically and was found to be ca. 30 wt %.

Colloidal Silica. Colloidal silica dispersions (30 wt % solids), Klebosol 30R25 (K-25) and Klebosol 30R50 (K-50), were supplied by Clariant Corp. The filler particles are amorphous spherical silica beads with diameters of 27 and 73 nm, respectively.

Colloidal silica dispersions (20 wt % solids), Snowtex-O (S-12) and Snowtex-OL (S-45), were supplied by Nissan Chemical Industries. These silica particles are also amorphous spherical beads with diameters of 16 and 54 nm, respectively. Both samples contain acidic small particles of silicasol, with a free anion content less than 300 ppm.[3] Further characteristics of these particles are shown in Table 2.

Particle Size Measurements. Dynamic light scattering (DLS) experiments were carried out on a variable angle laser light scattering photometer from Brookhaven Instruments Corp. A 5 mW vertically polarized He−Ne laser from Spectra Physics was the light source. The silica dispersion in water was filtered through disposable 0.45 μm Gelman filters into glass scattering cells. The cells were placed into the BI-200SM goniometer and sat in a vat of thermostated toluene that matched the index of refraction of the glass cells. The angular range of the goniometer was 7−162°. The scattered light was detected by a photomultiplier interfaced to the BI-2030AT digital correlator with 136 channels, and the correlation function was measured in real time. Dynamic light scattering data were analyzed following the method of cumulants.[9] Dynamic light scattering data were also analyzed using the CONTIN[10] method to examine the distribution of hydrodynamic size.

Transmission electron microscopy (TEM) measurements were carried out on a Hitachi model 600 electron microscope. The samples were prepared as follows. Thin carbon films (ca. 5 Å) were grown on mica as a support. Then 25 μL of the silica dispersion in water was added onto the carbon-coated mica surface. After the water was evaporated, each carbon film was floated off the mica support in water and deposited onto a 300 mesh Gilder copper grid. The sample was air-dried before introduction into the electron microscope. Staining of the sample was unnecessary. The diameter of the silica was measured directly from the TEM micrograph, using "Photoshop" software. For each sample, around 100−200 particles were measured, and the average was taken as the final diameter.

Film Formation and Measurements. Before we prepared films from the PBMA latex and colloidal silica dispersions, the latex and Klebosol dispersions were cleaned by treating the individual dispersions with a prepurified ion-exchange resin (AG-508-X8 mixed-bed resin, Bio-Rad) to remove the ionic surfactant and other ionic species. For each sample, the pH decreased from 8−9 to 2−3 after the ion exchange. The Snowtex dispersions were used as supplied. Latex films were prepared from dispersion mixtures with a 1:1 number ratio of Phe- and An-labeled PBMA latex particles and different amounts of silica. The final dispersions, with total solids content ranging from ca. 8 to 19 wt %, have pH = 3−4. Film formation was carried out by the following procedure. For each film, using a Pasteur pipet, we spread eight drops from each dispersion mixture onto a quartz plate. The film was allowed to dry over 40 min in an oven at 31 ± 1 °C, followed by storage in the cold room at 4 °C to minimize the amount of polymer interdiffusion in the film. A typical film thickness was 150 μm. Films formed from latex alone were crack-free and transparent. All of the other films were transparent and crack-free up to 30 wt %, but small cracks were observed in the films containing 40 wt % filler. It was hard to work with films containing above 40 wt % filler. All films were annealed at 60 ± 1 °C for polymer diffusion measurements. For each series of samples to be compared, the films were annealed simultaneously.

Fluorescence decay profiles were measured by the single photon-timing technique.[11] Samples were excited at 300 nm, and the emission was detected at 350 nm. A band-pass filter (350 ± 5 nm) was used to minimize the scattered light and interference due to fluorescence from excited acceptors. For each measurement, it took about 10 to 15 min to collect 5000 counts in the maximum channel. Prior to each measurement, a film sample was placed in a quartz tube, and the tube was degassed with flowing nitrogen gas.

Data and Data Analysis. We monitor the polymer diffusion process by measuring changes in the extent of energy transfer between the donor and acceptor dyes attached to these latex polymers. When a donor dye D is excited, it can transfer its energy to any nearby acceptor dyes A. The important feature of this process is that the rate of energy transfer, $w(r)$, depends sensitively on the distance r between the donor and acceptor molecules

$$w(r) = \frac{1}{\tau_D^0}\left(\frac{R_0}{r}\right)^6 \tag{1}$$

where τ_D^0 is the donor fluorescence lifetime in the absence of acceptors, and R_0 is the characteristic distance (the Förster distance) over which energy transfer takes place. [12] For energy transfer for donors and acceptors randomly distributed in a three-dimensional Euclidean space, the donor decay function, following instantaneous excitation at time $t' = 0$, will have a stretched exponential form[13]

$$I_D(t') = I_o \exp\left(-\frac{t'}{\tau_D}\right) \exp\left[-P\left(\frac{t'}{\tau_D}\right)^{0.5}\right] \tag{2a}$$

Table 2. Characteristics of the Latex and Colloidal Silica

		colloidal silica			
	An-PBMA[a]	Klebosol 30R25 (K-25)	Klebosol 30R50 (K-50)	Snowtex O (S-12)	Snowtex OL (S-45)
diameter (nm)		25[b]	50[b]	11−14[b]	40−50[b]
DLS[c]	90.8	25.6 (0.033)	73.1 (0.005)	11.6 (0.283)	74.8 (0.052)
TEM[d]	94.8	26.7 (2.6)	72.9 (4.0)	16.0 (3.5)	53.5 (13.7)
pH of dispersion[e]	7.8/3.4	9.0/3.0	9.0/3.0	3.5	3.3
conductivity (μS/cm)[e]	800/160	2000/300	1200/150	300	270

[a] M_w = 50 000, M_n = 20 000, T_g = 30 °C. The particle size, T_g, and molecular weight for Phe-PBMA are very similar to those for An-PBMA. [b] Obtained from the product brochures. [c] Mean diameters determined by dynamic light scattering (polydispersity). [d] Mean diameters determined by transmission electron microscopy (SD, nm). The standard deviation (SD) was calculated as $SD = ((1/n - 1)\sum (X_i - \bar{X})^2)^{1/2}$, where n is the sample size and $\bar{X}$ is the mean. [e] The pH values before/after ion-exchange are shown for PBMA latex and Klebosol silica.

where I_0 is the intensity at zero time and P is a parameter proportional to the local concentration of acceptors C_A

$$P = \kappa^2 \frac{4\pi^{3/2}}{3000} N_{Av} R_0^{\,3} C_A \tag{2b}$$

where N_{Av} is Avogadro's number and κ^2 describes the averaged relative orientation of the donor and acceptor dipole moments.

In our experiments, we measure donor fluorescence decay profiles $I_D(t')$. Some decay curves were fit to eq 2a. To fit most of the decay curves, we use the following phenomenological equation:

$$I_D(t') = A_1 \exp\left[-\frac{t'}{\tau_D^{\,0}} - p\left(\frac{t'}{\tau_D^{\,0}}\right)^{0.5}\right] + A_2 \exp\left(-\frac{t'}{\tau_D^{\,0}}\right) \tag{3}$$

While this equation is similar in form to eq 2a, no meaning is ascribed to the individual fitting parameters. The parameters A_1, A_2, and p are obtained from the fit of each decay profile, and we use these fitting parameters to integrate $I_D(t')$ analytically, from decay time t' = zero to t' = infinity.

The efficiency of energy transfer for a sample aged or annealed for a time t, $\Phi_{ET}(t)$, is defined as

$$\Phi_{ET}(t) = \frac{\text{number of ET events}}{\text{number of photons absorbed}} = 1 - \frac{\int_0^\infty I_D(t')\,dt'}{\int_0^\infty I_D^{\,0}\,dt'} \tag{4}$$

where the integral in the numerator is the area under the fluorescence donor decay profile obtained from the samples containing both D and A,[14] and that in the denominator is the unquenched donor lifetime τ_D^o. Equation 4 can be rewritten as

$$\Phi_{ET}(t) = 1 - \frac{\text{area}(t)}{\tau_D^{\,0}} \tag{5}$$

While the extent of energy transfer can in principle be determined by measuring the intensities of donor and acceptor fluorescence, this experiment suffers from several artifacts, particularly the absorption by A of light emitted by the excited D. In our experiments, we avoid this problem by carrying out fluorescence decay experiments. We measure the influence of the acceptor dye on the decay rate of the donor dye following pulsed excitation. In the absence of acceptor, the phenanthrene chromophore we employ as the donor dye undergoes an exponential decay with a lifetime τ_D^0. In our analysis of the donor fluorescence decay data, we assume that all deviations from a strictly exponential donor decay profile are due to FRET. For the films we examine here, τ_D^0 is approximately 45 ns.

Another useful parameter is the extent of mixing, $f_m(t)$, expressed in terms of the growth in energy transfer efficiency, normalized by the maximum change associated with complete mixing[14]

$$f_m(t) = \frac{\Phi_{ET}(t) - \Phi_{ET}(0)}{\Phi_{ET}(\infty) - \Phi_{ET}(0)} = \frac{\text{area}(0) - \text{area}(t)}{\text{area}(0) - \text{area}(\infty)} \tag{6}$$

where $[\Phi_{ET}(t) - \Phi_{ET}(0)]$ represents the change in the efficiency of energy transfer between the initially prepared film and a film annealed for time t.

Results

Determination of Silica Particle Sizes by DLS and TEM. In this paper, we examine the effect of silica particle size on the rate of polymer interdiffusion. Therefore, it is important to know the exact silica particle size. We employed both dynamic light scattering (DLS) and transmission electron microscopy (TEM) measurements to determine the particle size, and compared the data with those described in the product brochures.[3,15] The data are summarized in Table 2. The mean particle diameters determined by DLS and those described in the product brochures are very similar for K-25 and S-12, whereas for K-50 and S-45, the DLS analysis leads to much larger values. The DLS data, for the silica particles in the dispersed state, provide the volume average particle size (hydrodynamic radius), so that the larger particles are emphasized in the calculation. One can see that the polydispersity for S-12 is very large. On the other hand, K-50 is nearly monodisperse.

We also employed TEM measurements to determine the silica particle size. For each sample, approximately 100 to 200 particles were measured, and we calculated the number-averaged particle diameter. The particle size distributions for K-25 and K-50 are narrow. S-12 has a relatively broad unimodal distribution and S-45 has a very broad distribution. TEM images of these particles are presented in the M.Sc. thesis of Kobayashi.[16] The mean particle sizes and the standard deviations obtained from TEM analysis are collected in Table 2. The average particle sizes obtained by TEM for K-25, K-50, and S-12 are close to those obtained by DLS. Because of the relatively broad particle size distribution, the average particle size obtained by TEM for S-45 is much smaller than that obtained by DLS. In the following sections, when we discuss these particles, we will use the number-averaged diameters obtained by TEM.

Influence of Silica on FRET Measurements of the Polymer Diffusion Rate. In this study, we examine the influence of colloidal silica (SiO_2) as a filler on the rate of polymer interdiffusion. We compare four different types of SiO_2 with diameters ranging from 16 to 73 nm. Useful films could be prepared containing as much as 40 wt % (23.3 vol %) filler. When we attempted to prepare films containing larger amounts of silica, those films were so brittle after they dried that they

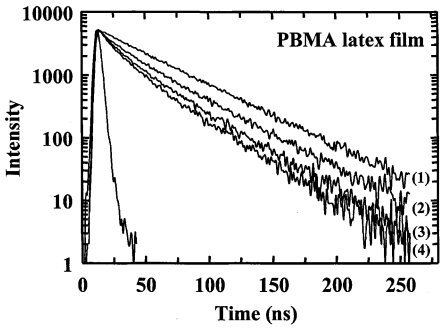

Figure 1. Donor fluorescence decay profiles in a PBMA latex film annealed at 60 °C for (1) 0, (2) 60, (3) 330, or (4) 12 000 min.

could not be handled. Typical donor fluorescence decay profiles for latex film samples at different stages of annealing are shown in Figures 1 and 2. Figure 1 shows data obtained for a latex film containing no silica filler. The corresponding decay traces obtained for films containing 40 wt % of silica of 16 nm (Snowtex-O, S-12), 27 nm (Klebosol 30R25, K-25), 54 nm (Snowtex-OL, S-45), and 73 nm (Klebosol 30R50, K-50, diameter are shown respectively in Figure 2, parts a−d. When these latex films were annealed at 60 °C, well above the polymer T_g (20 °C), polymer interdiffusion takes place. One can see the evolution of polymer interdiffusion in the films by looking at the extent of curvature of the decay profiles. As one anneals the film for longer times, the curvature becomes more pronounced, which indicates that polymer interdiffusion is promoted by heat and annealing time.

If one compares the curves in parts a and b of Figure 2 with those in Figure 1, one sees less curvature in the decay curves at comparable annealing times (at 60 °C) when silica is present in the sample. This result tells us that polymer diffusion is retarded over the entire annealing time. In the decay curves themselves, one can see that there is greater retardation of the diffusion rate in the samples containing smaller silica particles. For example, in parts a and b of Figure 2, one can see that the extent of energy transfer is strongly suppressed due to the smaller size of SiO_2. One can also see, in parts c and d of Figure 2, that the rate of polymer interdiffusion is retarded for the first several hours, but the $I_D(t)$ decay profiles reach an extent of curvature after 200 h of annealing at 60 °C similar to that shown in Figure 1.

To put these experiments in context, we note that Feng et al.[17] studied the effect of an organic filler (poly(methyl methacrylate), PMMA) on the rate of polymer interdiffusion in poly(butyl methacrylate) (PBMA) latex films. In their experiments, they examined films containing a constant fraction (35 vol %) of PMMA particles of different sizes. They found that the PBMA diffusion rate decreased in proportion to the increase in the surface area of the hard filler particles, i.e., with a decrease in the hard particle size at constant filler volume. On the basis of their results, we expected to see a larger effect on the polymer interdiffusion rate in the films containing smaller SiO_2, due to its much larger surface area.

In a previous study,[18] we examined the effect of two inorganic pigments on polymer interdiffusion in a low-T_g latex film. Calcium carbonate and colloidal silica were used as model inorganic pigments, and poly(methyl methacrylate-*co*-2-ethylhexyl acrylate) copolymer latex was used as the latex binder. In the case of micrometer-size precipitated calcium carbonate, only large amounts (>70 wt %), well above the critical pigment volume concentration (CPVC), retarded the rate of polymer interdiffusion. In contrast, the presence of much smaller silica particles significantly retarded the rate of polymer interdiffusion, even when the filler content was below the CPVC. In addition, the $\Phi_{ET}(\infty)$ values for the films containing large amounts of SiO_2 (e.g., 40 wt %) were much smaller than that for the film containing no SiO_2.

Efficiency of Energy Transfer $\Phi_{ET}(0)$ in Newly Formed Latex Films. In this section we examine the influence of filler on the extent of energy transfer in newly formed films. If these films are prepared at low enough temperature, little or no polymer interdiffusion will take place. Energy transfer will occur only across the interface between cells formed by the D- and A-labeled latex particles. Under these circumstances, $\Phi_{ET}(0)$ is a measure of the interfacial area between D- and A-labeled cells in the film.[17] The newly formed films we examined were allowed to dry uncovered in an oven at 31 ± 1 °C over 40 min, but as soon as each film appeared to be dry, it was transferred to the cold room at 4 °C for storage until the decay profile of the cold film could be measured. Since the T_g of the matrix polymer is ca. 20 °C, we imagine that minimal polymer diffusion occurs when the films are prepared in this way. In previous experiments on nascent films prepared from similar-sized latex particles at temperatures close to the minimum film forming temperature, $\Phi_{ET}(0)$ values on the order of 0.05−0.07 were obtained.[19] We take this as a value typical of that for intimate contact between latex polymers in adjacent cells of this size. Since we find $\Phi_{ET}(0) = 0.08-0.09$ in the silica-free films examined here (Figure 3), we conclude that little polymer diffusion occurs prior to the measurement of $\Phi_{ET}(0)$.

For films prepared in the presence of silica, the behavior is somewhat more complex. In Figure 3 we plot $\Phi_{ET}(0)$ vs SiO_2 content (wt %) for a series of freshly prepared films containing either K-25, K-50, S-12, or S-45. For the films containing K-50 and S-45, the $\Phi_{ET}(0)$ values hardly change with increasing silica content. For films containing K-25 and S-12, however, these values decrease with increasing silica content. Thus, these smaller particles are effective in reducing the amount of intercellular ET that occurs in the newly formed films.

Maximum Extent of Energy Transfer in PBMA Latex Films. To evaluate the extent of mixing, $f_m(t)$ defined by eq 10, we need to know the value of $\Phi_{ET}(\infty)$, which corresponds to full mixing of the polymer. If the film is fully mixed, one should have a random distribution of donors and acceptors, and the decay profile should be described by eq 2a. Under these circumstances, the rate and efficiency of energy transfer will be determined only by R_o, κ^2, and the concentration of acceptors in the film.

There are three ways to obtain a sample that will serve as a model for $\Phi_{ET}(\infty)$. First, one can take a film and anneal it for a sufficiently long time. Second, one can take a film and anneal it at high temperature. Since the polymer diffusion rate is strongly accelerated by increasing temperature, Φ_{ET} will normally increase rapidly to its maximum value. Finally, one can dissolve a dry film sample in an organic solvent. In solution, one expects full mixing of the polymer molecules. A film cast from this solution is then a good model for the determination of $\Phi_{ET}(\infty)$. We have found in the past, for filler-

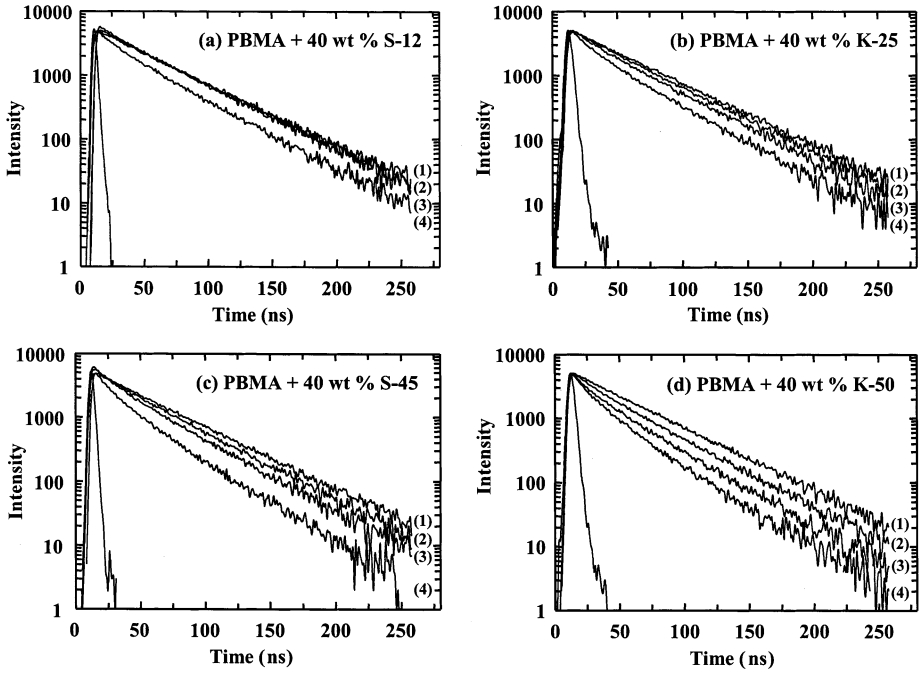

Figure 2. Donor fluorescence decay profiles in a PBMA latex film containing 40 wt % silica with average diameters of (a) 16 (S-12), (b) 27 (K-25), (c) 54 (S-45), and (d) 73 nm (K-50) annealed at 60 °C for (1) 0, (2) 60, (3) 330, and (4) 12 000 min, respectively.

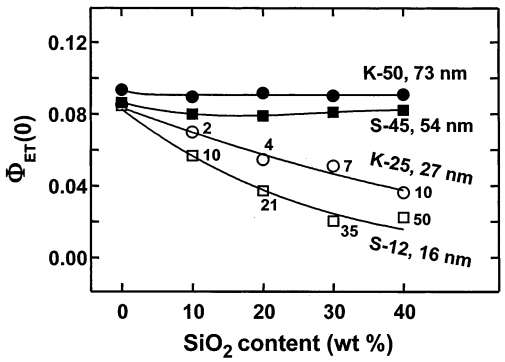

Figure 3. Plots of the initial efficiency of energy transfer, $\Phi_{ET}(0)$, vs SiO_2 contents in newly formed films. The numbers adjacent to the points on the lower two curves refer to the number ratio of silica-to-latex particles in the sample.

free films, that all these approaches give similar values of area(∞) from which the corresponding $\Phi_{ET}(\infty)$ values are calculated.[17] In this section, we examine the effect of filler on the magnitude of $\Phi_{ET}(\infty)$.

In the experiments reported here, we obtained area(∞) values for filler-free latex films, from a solvent-cast film. This film was prepared from a dry PBMA film prepared from a 1:1 mixture of D- and A-labeled particles, which was subsequently dissolved in tetrahydrofuran (THF). The solution was cast onto a quartz plate and allowed to dry at room temperature for 12 h. For these films, we obtained an area(∞) value of 14.5 ns and a $\Phi_{ET}(\infty)$ value of 0.68, and these values did not change when the film was annealed at 80 °C for 1 h. In contrast, when a sample of the latex film itself was annealed at 60 °C for 200 h, we obtained an area(∞) value of 16.1 ns and a $\Phi_{ET}(\infty)$ value of 0.65. One can see that a latex film heated at 60 °C for this length of time gave values close to those obtained from the solvent-cast film.

In this section, we describe results of experiments carried out on a series of samples that differ in their silica content. Since small variations in oven temperature can effect the rate of polymer diffusion, we subjected each series of samples to simultaneous annealing in the oven. Because the different series of samples were annealed at different times, one can expect small differences in the extent of mixing as a function of time. As a way of monitoring these differences, each sample set contains a film without silica. By comparing values of $\Phi_{ET}(t)$ for these samples, we can assess the effects of variation in oven temperature.

When films were prepared in the presence of filler and annealed for 200 h at 60 °C, we obtained values of area(200 h) and $\Phi_{ET}(200\ h)$ that depended on the amount of filler present. We determined area(200 h) and $\Phi_{ET}(200\ h)$ values for films containing up to 40 wt % of silica. For K-25, the values ranged from 16.6 (no silica) to 21.9 ns (40 wt % K-25), corresponding to $\Phi_{ET}(200\ h)$ values from 0.64 to 0.52. The SiO_2 filler has its most pronounced effect when it is present in amounts greater than 20 wt %. In the case of films containing S-12 filler, we see that $\Phi_{ET}(200\ h)$ values decrease with increasing amount of filler, following the same trend observed for films containing K-25. However, the magnitude of the decrease in $\Phi_{ET}(200\ h)$ for films containing S-12 is even larger than that for films containing K-25. The area(200 h) values ranged from 17.0 (no silica) to 31.6 ns (40 wt % S-12), corresponding to $\Phi_{ET}(200\ h)$ values from 0.63 to 0.30. Even the presence of a small amount of S-12 affects the $\Phi_{ET}(200\ h)$ values, and as the filler content is increased, it has an even larger effect on $\Phi_{ET}(200\ h)$ values. For K-50, the area(200 h) values ranged from 16.1 to 17.0 ns, corresponding to $\Phi_{ET}(200\ h)$ values from 0.64 to 0.62, and for S-45, these values ranged from 16.2 to 16.9 ns, corresponding to $\Phi_{ET}(200\ h)$ values from 0.64 to 0.63. Unlike the case of K-25 or S-12, the presence of these fillers does not lead to a lowering of $\Phi_{ET}(200\ h)$ values. These data are summarized in Table 3.

In summary, the presence of 54 or 73 nm diameter silica particles (K-50 and S-45) has almost no effect on the area(200 h) and $\Phi_{ET}(200\ h)$ values. The values we

Table 3. Φ_{ET}(200 h) at Different Annealing Temperatures

	Φ_{ET} at 60 °C		Φ_{ET} at 90 °C		Φ_{ET} at 120 °C	
	10 min	120 min	10 min	120 min	10 min	120 min
PBMA	0.24	0.45	0.63	0.66	0.65	0.66
PBMA + 40 wt % K-25	0.15	0.24	0.38	0.49	0.56	0.61
PBMA + 40 wt % K-50	0.22	0.42	0.57	0.65	0.66	0.65
PBMA + 40 wt % S-12	0.08	0.15	0.30	0.46	0.54	0.58
PBMA + 40 wt % S-45	0.20	0.34	0.56	0.65	0.65	0.64

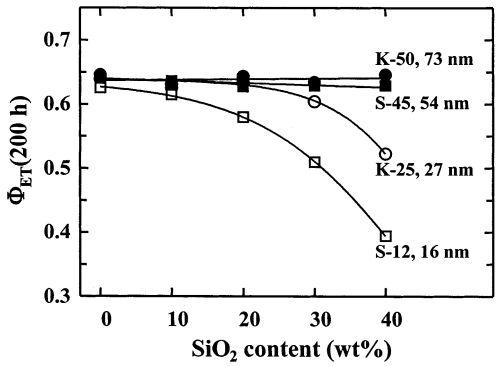

Figure 4. Plots of the efficiency of energy transfer for latex films annealed for 200 h at 60 °C, Φ_{ET} (200 h), vs SiO_2 content.

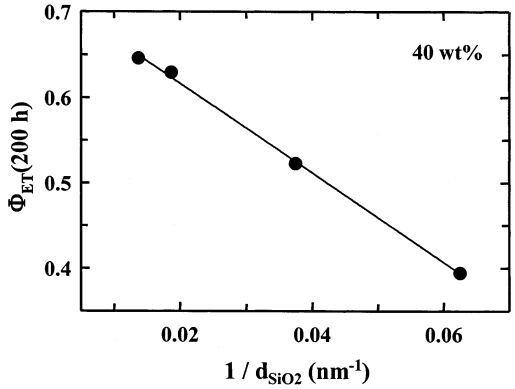

Figure 5. Plots of the efficiency of energy transfer Φ_{ET} (200 h) vs the surface-to-volume ratio ($1/d_{SiO_2}$). These films contain 40 wt % of SiO_2 and were annealed for 200 h at 60 °C. The mean diameters of the silica particles were determined by TEM.

calculate are almost identical to those in the filler-free film, where essentially full mixing of the donor- and acceptor-labeled polymer occurs. We conclude that these relatively large particles have little effect on the extent of polymer diffusion that takes place when the films were heated for 200 h at 60 °C. In contrast, we observe significant changes in area(200 h) and Φ_{ET}(200 h) values in latex films containing the smaller silica particles (K-25 and S-12). The results are summarized in Figure 4. Here the filler particles retard polymer diffusion to such an extent that the extent of mixing after 200 h annealing is significantly reduced. In Figure 5, we plot Φ_{ET}(200 h) values for films containing 40 wt % of SiO_2 annealed for 200 h at 60 °C, as a function of the inverse diameters of SiO_2. The number-average diameters of silica particles were determined by transmission electron microscopy (TEM). Since $1/d_{SiO_2}$ corresponds to the surface-to-volume ratio of SiO_2 filler, one can see that there is a linear relationship between Φ_{ET}(200 h) values and the calculated surface-to-volume ratio.

In Figure 6 we examine this effect from a different perspective, in which we annealed films containing 40 wt % (23.3 vol %) silica for 200 h at various temperatures. The Φ_{ET}(200 h) values increase with the annealing temperature, and approach 0.6 even in the presence of S-12 and K-25. These results indicate that interaction of the PBMA polymer with the surface of the silica particles slow the rate of polymer diffusion, but this interaction is not so strong as to suppress a part of the polymer mixing process.

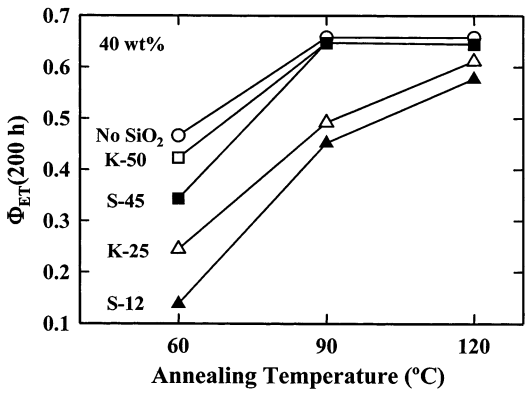

Figure 6. Plots of the efficiency of energy transfer, Φ_{ET} (200 h), vs annealing temperature. These films contain 40 wt % silica and were annealed for 200 h.

To examine the influence of pigment on the rate of polymer interdiffusion, we need to introduce values of area(∞) or $\Phi_{ET}(\infty)$ into the calculation of $f_m(t)$. Since $f_m(t)$ is a measure of the extent of mixing in the PBMA/silica system, we need to determine both area(∞) and $\Phi_{ET}(\infty)$ values that describe only the latex polymer in the system, so that we can consider separately the effect of filler on the rate and the total extent of polymer diffusion. For this reason, we use values obtained for the filler-free polymer obtained by solvent casting, area(∞) = 14.5 ns, and $\Phi_{ET}(\infty) = 0.68$, in the calculation of all f_m values.

Effect of Silica Particle Size on the Rate of Polymer Interdiffusion. In this section, we examine the influence of silica on the rate of polymer diffusion in PBMA latex films. The $f_m(t)$ values were calculated with eq 6 from the areas under the fluorescent decay curves, using area(0) values corresponding to each film, but a common area(∞) value of 14.5 ns. In Figure 7, we plot values of $f_m(t)$ as a function of annealing time at 60 °C for films containing different amounts of silica. In Figure 7a, we see that the presence S-12 in the film has a significant effect on reducing the rate of polymer interdiffusion. Even in the latex film with 10 wt % silica, it is obvious that S-12 retards the rate of polymer interdiffusion. There is greater retardation as one increases the amount of S-12 in latex films. When one increases the amount of S-12 in the latex film up to 40 wt %, one can see a significant effect of retardation on the polymer diffusion rate. In Figure 7b, we see that the presence of K-25 in the film has also a pronounced effect on reducing the rate of polymer interdiffusion, but less than that of S-12. Polymer interdiffusion is retarded by the presence of the S-45 and K-50 filler, but the

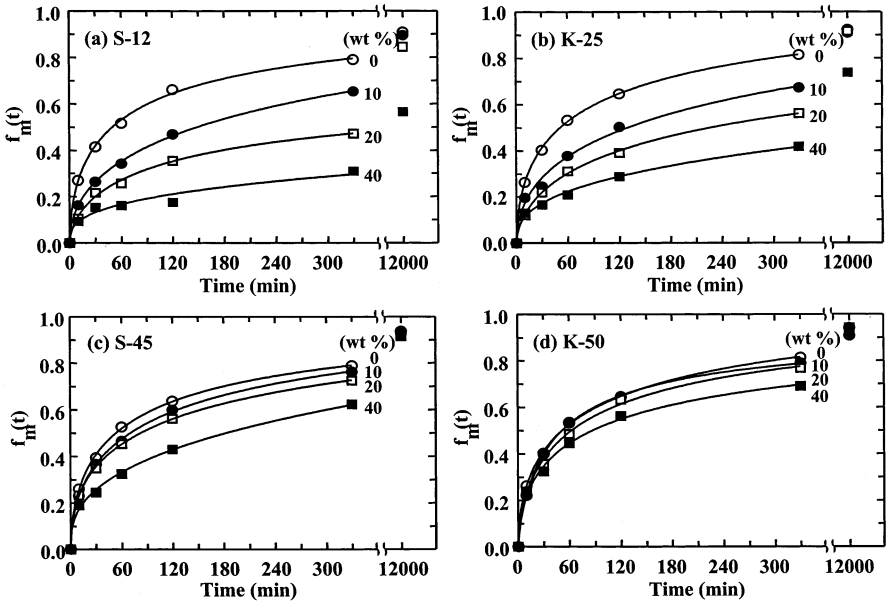

Figure 7. Plots of the extent of mixing $f_m(t)$, as a function of annealing time. Films were annealed simultaneously at 60 °C and contain different amounts of (a) 16 (S-12), (b) 27 (K-25), (d) 54 (S-45), and (c) 73 nm (K-50) silica.

extent of retardation is much smaller than that of S-12 or K-25.

Discussion

Films formed from a mixture of film-forming latex particles and silica particles share many features in common with hard−soft latex blend films. In both instances, the soft component will deform under the influence of forces associated with drying to form a film in which the soft component serves as a binder for the hard particles in the blend.[20] As the water evaporates, the mean spacing between particles decreases. The viscosity mounts, retarding and eventually suppressing particle motion. The morphology of the film that is formed reflects the distribution of the components in the aqueous phase at high solids.

There is a lot of interest in morphological features of films formed from bimodal latex blends. A number of authors have examined films formed from blends of large and small latex particles, whereas we[21] and others[22,23] have examined films formed from blends of hard and soft latex. The major factors that affect the particle distribution in these films are reviewed in a recent contribution from the Keddie group.[24] One of the most important concepts is that of phase continuity.[25] In our blends, the films undergo a transition from pliant to brittle when the hard component forms the continuous phase. The minimum volume fraction of small particles that is required to achieve a continuous phase is defined as the critical volume fraction V_c. The magnitude of V_c depends on the ratio of particle diameters and how the particles pack in the film. To give perspective to their experiments on latex films formed from binary mixtures of large and small particles, Tzitzinou et al.[24] model the case in which the small particles form a continuous hexagonally packed phase around each of the larger primary particles. For the 6:1 particle size ratio they examined, $V_c = 0.18$. The situation is more complicated if either component has a broad size distribution or if the minor component tends to aggregate as the dispersion dries. Eckersley and Helmer[26] have shown that in blends of hard small latex particles with large soft latex particles, careful control of the particle size ratio provides good film formation coupled with enhanced mechanical properties and block resistance.

In the system we describe, the soft PBMA component always forms the continuous phase. Because the films are transparent, we infer that there is no tendency for the silica to form large aggregates that would by themselves scatter light and induce turbidity, or to create large voids. Our energy transfer experiments provide further insights into features of the detailed morphology of these films.

$\Phi_{ET}(0)$ in Newly Formed PBMA Latex Films in the Presence and Absence of Silica. For polymers to diffuse between cells in a latex film, the individual particles must deform sufficiently to come into intimate contact. Ideally, this deformation and wetting will occur on a faster time scale than the polymer diffusion step,[27] so that these two processes can be studied separately. In the absence of intercellular diffusion, ET can take place only between donors and acceptors on opposite sides of the boundary between adjacent cells. Under these circumstances, the efficiency of energy transfer in a newly latex formed film, $\Phi_{ET}(0)$, provides a measure of the interfacial area of intimate contact between D- and A-labeled latex cells.[17] Since the characteristic distance for ET between Phe and An is so small, any factor that prevents local contact between these cells will reduce or prevent ET in that part of the film. As one can see in Figure 3, $\Phi_{ET}(0)$ values decrease with increasing amount of K-25 and S-12, whereas those of K-50 and S-45 are constant.

Two factors can contribute to the decrease in $\Phi_{ET}(0)$. The first is the presence of microvoids. As described by Keddie et al., [28] voids with nanometer dimensions are too small to cause film turbidity but can be detected by ellipsometry as a mean index of refraction smaller than that expected for a dense film. These voids are most easily detected in films formed within 10 °C of the polymer glass transition. Because of the slow viscoelastic relaxation rate of the polymer under these conditions, the voids take a long time to disappear.

The second is the presence of "foreign matter" such as surfactant or pigment particles that occupy the space

between adjacent cells of donor- and acceptor-labeled polymer. The influence of silica particles on the magnitude of $\Phi_{ET}(0)$ will depend on the number and size ratios of the silica to latex particles and how the particles pack in the film. For the hexagonal packing considered by Tzitzinou et al.,[24] V_c corresponds to the case where the small particles completely surround the large particles, and its magnitude depends only on the ratio of the particle diameters. If this type of packing occurred in the systems we examined, then at V_c, $\Phi_{ET}(0)$ would drop to zero. For example, $V_c = 0.18$ for a particle diameter ratio of 6, corresponding roughly to the highest content of the S-12 particles shown in Figure 3.

Below V_c, for a given weight fraction of silica in the blend, small particles would be more effective than large particles in covering the surface of individual latex cells. The important parameter describing this effect should be the number ratio of silica to latex particles. To illustrate this result, we indicate in Figure 3 selected values of the number ratio (calculated from the mean silica particle diameters) of silica-to-latex particles. For the 27 and 16 nm diameter silica, these numbers ranges from 2 to 44. One can see that the decrease in $\Phi_{ET}(0)$ is associated with the larger particle ratios, but this is not the whole story. Kusy has emphasized that that "for phase continuity to occur, the dispersed particles, which contact a primary particle, need cover only a fraction of the primary particle surface."[25] Under these circumstances, even at V_c, $\Phi_{ET}(0)$ would not necessarily be equal to zero. Other factors that may play a role include, for example, particle size polydispersity, particularly in the S-12 sample, or a tendency for the silica (or latex) to form small clusters or aggregates as the dispersion dries. We conclude that the small silica particles are effective at reducing the interfacial contact area between D- and A-labeled latex cells but that this effect does not depend only on the number fraction of small particles in the blend.

Effect of Silica on Φ_{ET}(200 h). In the absence of silica, when latex films are annealed for long periods of time, polymer diffusion leads to complete mixing of D- and A-labeled polymer. In the presence of silica, we see a pronounced reduction in the extent of mixing in films containing 20 to 40 wt % of the small silica particles S-12 and K-25. As one sees in Figure 4, after 200 h annealing at 60 °C, substantial amounts of polymer remain unmixed, leading to decreased values of Φ_{ET}(200 h). To explain this effect, we imagine that the polymer adjacent to the particle surface is adsorbed to the silica. The Si−OH groups at the surface of the silica are likely to be strong hydrogen bond donors toward the ester groups of the PBMA. Adsorbed polymer would require either very long times or elevated temperatures to desorb. In accord with this idea, we found, in Figure 6, that after 200 h annealing at 120 °C, Φ_{ET} values for films containing 40 wt % S-12 or K-25 approached the value expected for complete interdiffusion of the latex polymer. The larger particles S-45 and K-50 had a much smaller influence on the magnitude of Φ_{ET}(200 h). The plot in Figure 5 suggests that the magnitude of this effect is related almost entirely to the difference in surface-to-volume ratio for these filler particles.

Analysis of the Diffusion Process. In this section, we analyze the $f_m(t)$ data more deeply to try to understand how mineral fillers affect the polymer molecules as they diffuse across the latex cell boundaries. If the diffusion follows Fick's laws, one expects that the extent of mixing $f_m(t)$ will be proportional to the square root of time.[29] We plot $f_m(t)$ as a function of $t^{1/2}$ in Figure 8. These plots are linear for values of $f_m(t)$ up to 0.7 for the film without silica. In addition, the films containing different sizes of SiO_2 filler also give reasonable linear plots. We fit each series of data to a straight line and note that they all have a small positive intercept. In the analysis described below, we only consider the slopes obtained by the least-squares best fits to the lines shown in Figure 8 and ignore the intercepts at $t = 0$ (with $f_m(t) \leq 0.06$). The slope of each line is a measure of the polymer mobility in the film. To examine how the surface-to-volume ratio of the silica particles affects this mobility, we plot the values of the slopes ($f_m(t)/t^{1/2}$) against $1/d_{SiO_2}$ in Figure 9. The data fall on a smooth curve, but not a straight line. When Feng et al.[17] examined the influence of PMMA particles as fillers on the rate of polymer diffusion in latex films, they found a linear dependence of ($f_m(t)/t^{1/2}$) on $1/d_{SiO_2}$. In their experiments, the filler content was kept constant at 35 vol %, and the particles had a narrow size distribution.

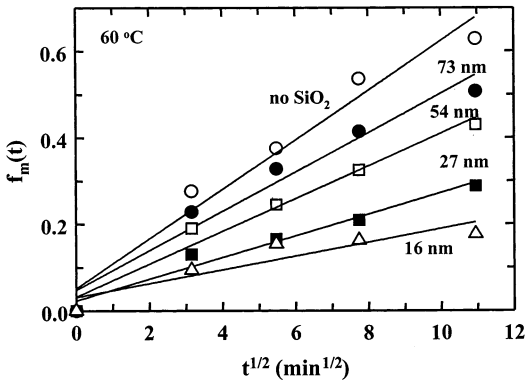

Figure 8. Plots of the extent of mixing $f_m(t)$, vs the square root of annealing time. The films contain 40 wt % of silica and were annealed at 60 °C.

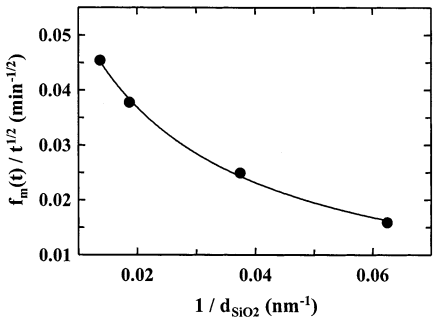

Figure 9. Plots of the values of the slopes in Figure 8 as a function of the surface-to-volume ratio, $1/d_{SiO_2}$ for 40 wt % (23.3 vol %) silica filler. The mean diameters of the silica were determined by TEM.

Calculating "Apparent" Diffusion Coefficients. Another measure of polymer mobility is the apparent diffusion coefficient D_{app}, which describes the rate of movement of the polymer molecules across the polymer−polymer interface between adjacent cells in the film.[30−32] We calculate these values by fitting the extent of mixing $f_m(t)$, obtained from the energy transfer measurements, to a spherical diffusion model which satisfies Fick's laws of diffusion, where D_s is the true diffusion coefficient.[33]

$$\frac{\partial C(r,t)}{\partial t} = \frac{1}{r^2}\frac{\partial}{\partial r}\left(D_s r^2 \frac{\partial C(r,t)}{\partial r}\right) \qquad (7)$$

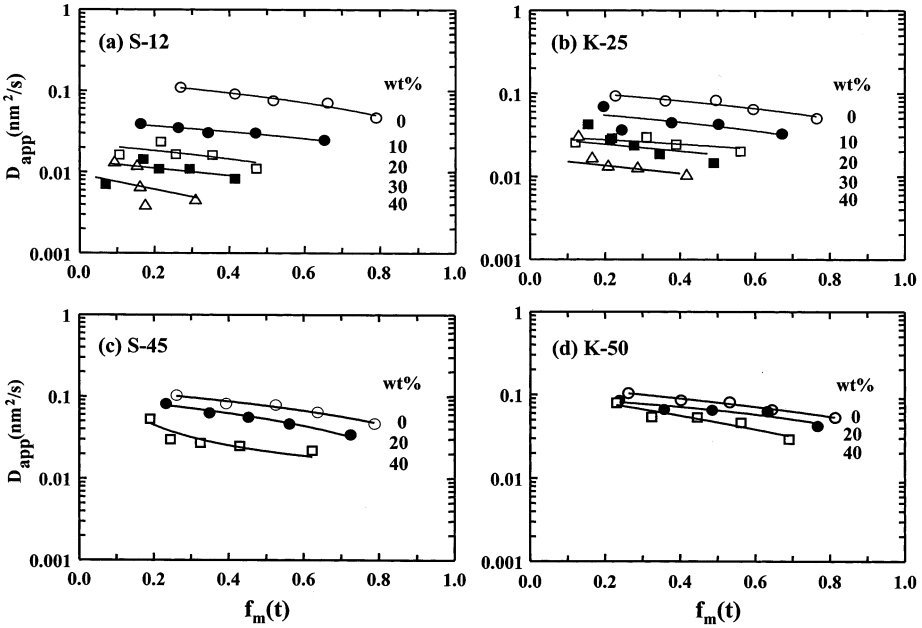

Figure 10. Mean apparent diffusion coefficients, D_{app}, as a function of the extent of mixing $f_m(t)$ for films containing (a) 16 (S-12), (b) 27 (K-25), (c) 54 (S-45), and (d) 73 nm (K-50) silica. The films were annealed simultaneously at 60 °C for each series of samples.

This model assumes that the diffusing substance is initially distributed uniformly in a sphere of radius R with an initial concentration C_0.[34] At time t we have

$$C(r,t) = \frac{C_0}{2}\left[\mathrm{erf}\left(\frac{R+r}{2\sqrt{Dt}}\right) + \mathrm{erf}\left(\frac{R-r}{2\sqrt{Dt}}\right)\right] - \frac{C_0}{r}\sqrt{\frac{Dt}{\pi}}\left\{\exp\left[-\frac{(R-r)^2}{4Dt}\right] - \exp\left[-\frac{(R+r)^2}{4Dt}\right]\right\} \quad (8)$$

D_{app} values are calculated by equating f_m with the fractional mass f_s which has diffused across the interface, $f_s = M_t/M_\infty$, where $M_\infty = (4/3)\pi R^3 C_0$, and carrying out a numerical integration to find the best D_{app} value which satisfies the equation

$$M_t = M_\infty - \int_0^R C(r)(4\pi r^2)\,\mathrm{d}r \quad (9)$$

Simulations have shown[35] that for the particle size and concentration of acceptor employed here, $f_m(t)$ increases more rapidly than $f_s(t)$. Thus, values calculated for D_{app} are larger than those for D_s. The simulations also show that D_{app} is proportional to D_s for values of $f_m(t)$ up to 0.7, and in this range the two D values differ by a factor of 3.

Experiments on latex films involve polymers with a distribution of chain lengths and a corresponding distribution of D_s values. The D_{app} values we obtained are apparent mean diffusion coefficients averaged over all the chain lengths in the sample latex polymer and the annealing history of the film.[17] Previous experience[36] has shown that molecular weight polydispersity leads to D_{app} values that decrease with increasing $f_m(t)$.[31] The short chain polymers dominate the initial polymer diffusion. At longer times, the growth in $\Phi_{ET}(t)$ and $f_m(t)$ is due to the diffusion of longer chain polymers. Because D_{app} values vary with $f_m(t)$, values of D_{app} from separate experiments should be compared at similar extents of mixing.

In Figure 10, we plot values of D_{app} as a function of $f_m(t)$ for films containing different amounts of silica. Figure 10a shows that the presence of 20 wt % S-12 in the film has a pronounced effect on reducing the rate of polymer interdiffusion. We compare the D_{app} values at $f_m(t) \approx 0.31$. The D_{app} value decreases from 0.10 nm^2/s for the film containing no silica, to 0.016 nm/s^2 for the film containing 20 wt % S-12 and to 0.004 nm/s^2 for the film containing 40 wt % S-12. When one increases the amount of S-12 in the latex film up to 40 wt %, one can see a significant effect of retardation. However, the difference in D_{app} values appears to be greater between the film with 0 and 20 wt % filler than those between 20 and 40 wt %. The same trend is observed in Figure 10b where we compare the D_{app} values at $f_m(t) \approx 0.35$ for K-25. One sees that the D_{app} value decreases from 0.081 nm/s^2 for the film containing no silica, to 0.027 nm/s^2 for the film containing 20 wt % K-25 and to 0.011 nm/s^2 for the film containing 40 wt % K-25. As in the case of S-12, we see that the presence of K-25 in the film has a significant effect on reducing the rate of polymer interdiffusion.

In Figure 10c, we plot D_{app} values as a function of $f_m(t)$ for films containing different amounts of S-45. Polymer interdiffusion is retarded by the presence of S-45 filler, but the extent of retardation is much smaller than that of S-12 or K-25. The D_{app} values compared at $f_m(t) \approx 0.50$ decrease from 0.078 nm/s^2 for the film containing no silica to 0.030 nm/s^2 for the film containing 20 wt % S-45 and to 0.023 nm/s^2 for the film containing 40 wt % S-45. In Figure 10d, we plot values of D_{app} as a function of $f_m(t)$ for films containing different amounts of K-50. D_{app} values do not change much with increasing amount of K-50 filler.

In Figure 11, we plot $f_m(t)$ as a function of $t^{1/2}$ for films containing (a) S-12 and (b) K-25. As we described in the previous section, all of the data give reasonable linear plots, indicating that polymer diffusion follows the Fick's laws even in the presence of silica particles. The slopes decrease as one increases the amount of silica, and the same trend can be seen for films containing different sizes of SiO_2. We plot those slope values as a function of silica volume fraction. We assume that the density

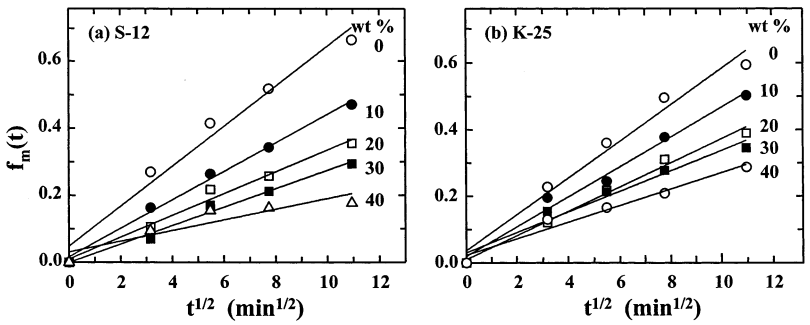

Figure 11. Plots of the extent of mixing $f_m(t)$ vs the square root of annealing time for latex films containing different amounts of (a) S-12 and (b) K-25 silica, annealed at 60 °C.

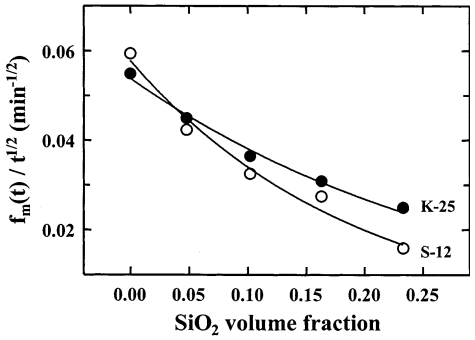

Figure 12. Plots of the slope values in parts a and b of Figure 11, as a function of the silica volume fraction.

of silica is 2.2 g/cm^3. One can see in Figure 12 that when the slope values are plotted against silica volume fraction, we obtain smooth curves but not straight lines.

Modeling the Influence of Silica on Polymer Diffusion. There are two types of explanations for the effect of filler particles on reducing the polymer diffusion rate as seen in Figures 9−12. On one hand, small particles can act as obstacles to increase the tortuosity of the diffusion path without affecting the friction that controls the rate of local diffusion. On the other hand, a hard pigment surface can make the adjacent polymer matrix more rigid. This is the traditional "filler effect" in which filler particles increase the modulus of elastomers. It is well-known that polymer chains adjacent to a strongly interacting rigid surface have decreased mobility.[37]

Tsagaropoulos and Eisenberg[38] examined the influence of small silica filler particles on tan δ determined from dynamic mechanical (DMA) measurements. As increasing amounts of filler were added, a new high glass transition temperature (T_g) was found in addition to the T_g for the bulk polymer. As more filler was added, they found a decrease in the magnitude of the DMA signal from which T_g was determined. They proposed a three-layer model of polymer mobility, with the layer immediately adjacent to the silica so rigid as to make no contribution to the DMA response. This layer was seen as separated from the unaffected bulk polymer by a layer of increased T_g. From this perspective, one reason for the decreased rate of polymer diffusion found here is that the polymer molecules near the filler surface have decreased mobility. Supporting this idea is our observation of the influence of silica particles on Φ_{ET}-(200 h) values in PBMA latex films. These results indicate to us that polymer adsorption onto the surface of the silica plays an important role in affecting the diffusion rate of the polymer in the filled systems.

For this reason, we examine how models based upon free volume are able to explain the observations that the presence of silica in PBMA latex films reduces the rate of polymer diffusion. Polymer diffusion rates, like most viscoelastic properties of polymers, exhibit a strong dependence on factors such as temperature, polymer molecular weight, and the presence of added low molecular weight diluents.[39] Viscoelastic properties of polymers can be well described by the Williams−Landel−Ferry (WLF) equation.[40] This equation describes temperature effects above the T_g of the polymer on dynamic properties of polymers related to backbone motions in terms of changes in the free volume in the system. This equation is based on the idea of time−temperature superposition. Events that occur on one time scale at a given temperature T occur on a faster time scale at higher temperatures. In the traditional WLF analysis, one defines a shift factor $a_T = t/t_r$, in terms of the shift along the time axis needed to bring two curves, representing measurements at different T, into correspondence at a reference temperature T_r. For diffusion coefficients, the WLF equation is written

$$\log a_T = \frac{-C_1(T - T_r)}{C_2 + T - T_r} = \log\left(\frac{DT_r}{D_r T}\right) \qquad (10)$$

where C_1 and C_2 are parameters characteristic of a particular polymer, and D_r is the diffusion coefficient determined at the reference temperature. In a study of the creep compliance of PBMA, Ferry and co-workers[41] were able to fit the data with $T_r = 373$ K, $C_1 = 14.5$, and $C_2 = 255$ K. Those values were found to be independent of molecular weight for PBMA samples of $M_w > 6.0 \times 10^4$.

In our approach to data analysis, we shift plots of the apparent diffusion coefficient D_{app} vs the extent of mixing $f_m(t)$ along the D-axis at constant T to bring the curves into correspondence at zero silica content ($\Phi_f = 0$). Thus, we can define a shift factor b_T as

$$b_T = \left(\frac{D_p(T,0)}{D_p(T,\Phi_f)}\right) \qquad (11)$$

where $D_p(T,\Phi_f)$ is the diffusion coefficient in the presence of an additive of volume fraction Φ_f, (here silica), and $D_p(T,0)$ is its magnitude in the pure polymer. Through the shift factor b_T, we introduce free volume theory, assuming that molecular transport as described by D_{app} is regulated by the availability of free volume in the system.[42] This shift factor is similar in form to that employed in the Fujita−Doolittle expression, an equation derived to explain the influence of low molec-

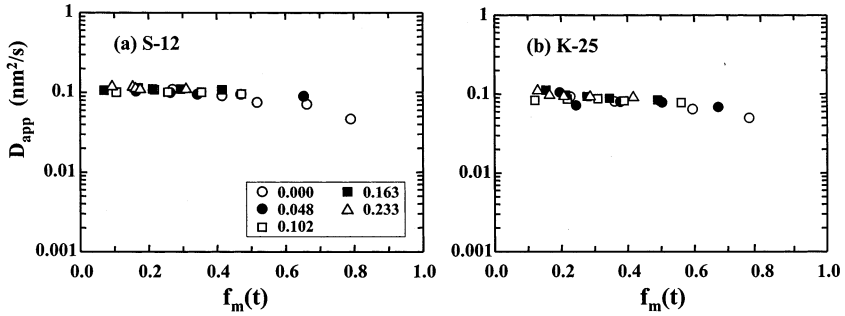

Figure 13. Master curve of D_{app} vs $f_m(t)$ for PBMA latex films containing (a) S-12 and (b) K-25. The volume fractions represented by each of the symbols are indicated in the inset in part a.

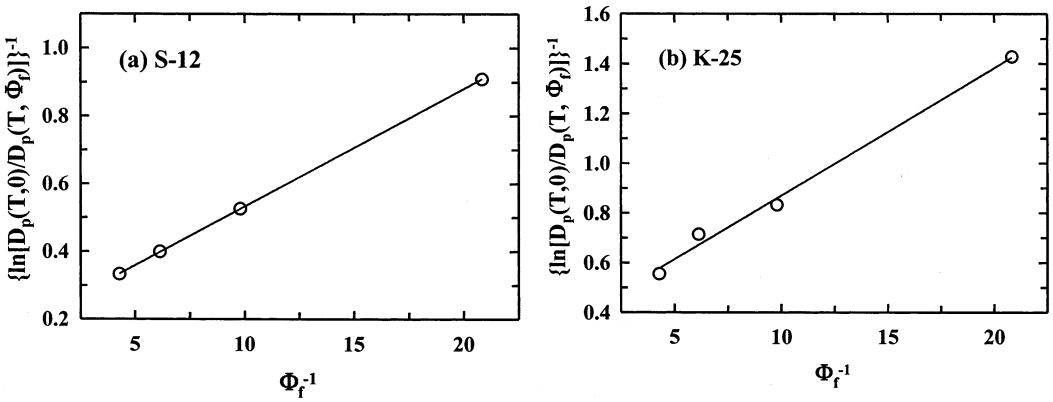

Figure 14. Plot of $\{\ln[D_p(T,0)/D_p(T,\Phi_f)]\}^{-1}$ vs Φ_f^{-1} for PBMA latex films containing various fractions of (a) S-12 and (b) K-25 silica.

ular weight plasticizers on the rates of plasticizer and polymer diffusion in their mixtures.

The Fujita−Doolittle equation is written as

$$\left(\ln\frac{D_p(T,\Phi_f)}{D_p(T,0)}\right)^{-1} = f_p(T,0) + \frac{f_p^2(T,0)}{\beta(T)\Phi_f} \qquad (12)$$

where Φ_f refers specifically to the amount of a soluble additive such as a plasticizer in the polymer. The term $f_p(T,0)$ refers to the fractional free volume in the polymer in the absence of additive and $\beta(T)$ is the difference in free volume between the additive and the polymer. Since small molecule plasticizers have more free volume than the polymer matrix, $\beta(T)$ is a positive number.

In our analysis, we assume that the silica particles act to rigidify the surrounding matrix, but they are not solutes in the traditional sense. If for the sake of argument we assume that silica particles act as an "antiplasticizer," we can obtain a mathematical relationship between the ratio of diffusion coefficients and the volume fraction of silica filler. To examine this idea, we equate D_{app} with $D_p(T,0)$ in the absence of silica, and with $D(T,\Phi_f)$ in the presence of S-12 and K-25. Since the plots of D_{app} vs $f_m(t)$ in Figure 10, parts a and b, are overall parallel for all sets of data, the values of $\{\ln[D_p(T,0)/D_p(T,\Phi_f)]\}^{-1}$ are essentially constant at different $f_m(t)$ values. Consequently all the data can be superimposed, and we obtain single master curves of D_{app} vs $f_m(t)$ for PBMA latex films containing different amounts of S-12 in Figure 13a and of K-25 in Figure 13b.

In Figure 14, we plot values of $\{\ln[D_p(T,0)/D_p(T,\Phi_f)]\}^{-1}$ vs Φ_f^{-1} for PBMA latex films containing various amounts of (a) S-12 and (b) K-25. We obtain straight lines, which indicates that the shift factor is a simple function of the silica volume fraction. The intercept is 0.19 and the slope is 0.035 in Figure 14a for the PBMA latex films containing S-12. For the PBMA latex films in Figure 14b containing K-25, the intercept is 0.36 and the slope is 0.051. If we plot $\{\ln[D_p(T,\Phi_f)/D_p(T,0)]\}^{-1}$ vs Φ_f^{-1}, as in eq 12, we also obtain straight lines with a negative slope. The plot also has a negative intercept. Too strict an adherence to the Fujita−Doolittle model would lead to the strange conclusion that $f_p(T,0)$, the free volume in the polymer in the absence of additive, is negative. In a plasticized polymer, the presence of the plasticizer adds free volume to the system and lowers T_g. In the silica-filled system, the filler particles rigidify the matrix surrounding each particle, and reduce the free volume of the system. Since the silica particles do not dissolve in the polymer, one cannot simply apply the Fujita−Doolittle model to our system.

Another way of analyzing these data is to assume that the filler changes the effective glass transition temperature of the polymer. Our data are not sufficiently rich for us to treat the situation described by Tsagaropoulos and Eisenberg[30] in which the filler surface raises T_g in the vicinity of the surface, with a smaller effect far removed from the surface. Here we assume that the presence of the silica increases the T_g of the entire matrix by an amount ΔT_g, and that this in turn increases the reference temperature employed in the WLF equation from T_r to $(T_r + \Delta T_g)$.

Equation 17 can be rewritten as

$$\log\left[\frac{DT_r}{TD_r}\right] = \frac{-C_1(T-(T_r+\Delta T_g))}{C_2 - T - (T_r + \Delta T_g)} \qquad (13)$$

The data fit well to this expression. As shown in Figure 15, ΔT_g values calculated in this way are a smooth

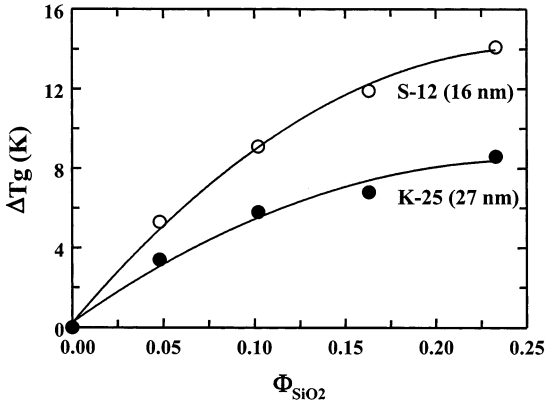

Figure 15. Plots of ΔT_g vs the silica volume fraction for PBMA latex films containing S-12 and K-25.

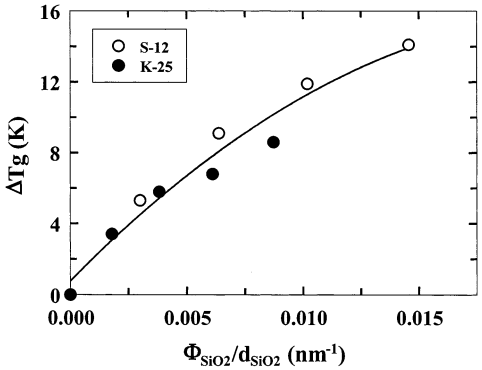

Figure 16. Plots of ΔT_g vs the ratio of the silica volume fraction divided by d_{SiO_2} for PBMA latex films containing S-12 and K-25.

increasing function of the silica volume fraction. Even more interesting is that when these data are normalized to a constant surface-to-volume ratio (Figure 16), both sets of data fall on a common line. This result provides strong support for the idea that the silica particles act to rigidify the surrounding matrix and that this effect can be effectively described by eq 13.

Conclusions

We employed the fluorescence resonance energy transfer (FRET) technique to measure the rate of polymer interdiffusion in PBMA latex films in the presence of colloidal silica, which has a large surface-to-volume ratio. The initial efficiency of energy transfer is constant in the presence of different amounts of 73 and 56 nm silica, but it decreases with increasing amounts of 16 and 27 nm diameter silica. This result indicates that 16 and 27 nm SiO_2 particles reduce the interfacial area between donor- and acceptor-labeled particles in the newly formed film. The extent of retardation in latex films with 73 nm SiO_2 is small, whereas that of 16 and 27 nm SiO_2 is much more pronounced on slowing the rate of polymer interdiffusion. The mean apparent diffusion coefficient (D_{app}) of the latex film with 16 nm SiO_2 (40 wt %) is 10 times smaller than that of the latex film without filler. The retarding effect of silica on the rate of polymer diffusion could be described quantitatively in terms of a model in which the presence of the silica leads to an increase in the T_g of the matrix. The increase in T_g is treated as an increase in the reference temperature T_r employed in the WLF equation to describe the influence of temperature on the rate of polymer diffusion. This increase in T_g means that experiments carried out at constant temperature are also carried out at decreased values of $(T - T_g)$.

Acknowledgment. The authors thank the Surface Science Consortium at the Pulp and Paper Centre, University of Toronto, and NSERC Canada, for their financial support and Clariant Corporation and Nissan Chemical Industries for kindly supplying the colloidal silica dispersions. M.K. thanks Oji Paper Co., Ltd., for his stay in Toronto.

References and Notes

(1) (a) Kraus, G. *Rubber Chem. Technol.* **1978**, *51*, 297. (b) Rharbi, Y.; Cabane, B.; Vacher, A.; Joanicot, M.; Boue, F. *Europhys. Lett.* **1999**, *46*, 472.
(2) Bourgeat-Lami, E.; Lang, J. *J. Colloid Interface Sci.* **1998**, *197*, 293.
(3) "SNOWTEX" Brochure; Nissan Chemical Industries, 1997.
(4) Imai, T.; Miyake, J.; Nojima, K. U.S. Patent 5,275,846, 1994.
(5) (a) Asano, S.; Ohashi, H.; Kondo, H.; Nojima, K.; Imabeppu, K.; Sakaki, M.; Suzuki, E. U.S. Patent 5,952,051, 1999. (b) Ogawa, S.; Senoh, H.; Andoh, M.; Nomura, H. U.S. Patent 5,750,200, 1998. (c) Imabeppu, K.; Asano, S.; Ohashi, H.; Nojima, K.; Suzuki, E.; Sakaki, M. U.S. Patent 5,741,584, 1998. (d) Asano, S.; Ohashi, H.; Kondo, H.; Nojima, K.; Imabeppu, K.; Sakaki, M.; Suzuki, E. U.S. Patent 5,670,242, 1997. (e) Ogawa, S.; Senoh, H.; Andoh, M.; Nomura, H. U.S. Patent 5,576,088, 1996.
(6) Feng, J.; Winnik, M. A. *Macromolecules* **1997**, *30*, 4324.
(7) Feng, J. Ph.D. Thesis, University of Toronto, Toronto, Canada, 1997.
(8) Brandrup, J.; Immergut, E. H. *Polymer Handbook*; Wiley: New York, 1989.
(9) Koppel, D. E. *J. Chem. Phys.* **1972**, *57*, 4814.
(10) Provencher, S. W. *J. Chem. Phys.* **1976**, *64*, 2772.
(11) O'Connor, D. V.; Phillips, D. *Time-correlated Single Photon Counting*; Academic: New York, 1984.
(12) (a) Wang, Y.; Kats, A.; Juhué, D.; Winnik, M. A. *Langmuir* **1992**, *8*, 1435. (b) Winnik, M. A. The Formation and Properties of Latex Films. In *Emulsion Polymerization and Emulsion Polymers*; Lovell, P. A., El-Aasser, M. S., Eds.; Wiley: New York, 1997. (c) Keddie, J. L. *Mater. Sci. Eng.* **1997**, *21*, 101.
(13) (a) Förster, Th. *Ann. Phys. (Leipzig)* **1948**, *2*, 55. (b) Lakowicz, J. R. *Principles of Fluorescence Spectroscopy*; Plenum Press: New York, 1983.
(14) (a) Wang, Y.; Zhao, C.; Winnik, M. A. *J. Chem. Phys.* **1991**, *95*, 2143. (b) Wang, Y.; Winnik, M. A.; Haley, F. *J. Coat. Technol.* **1992**, *64*, 51. (c) Kim, H.; Wang, Y.; Winnik, M. A. *Polymer* **1994**, *35*, 1779. (d) Kim, H.; Winnik, M. A. *Macromolecules* **1994**, *27*, 1007.
(15) "Klebosol" Brochure; Clariant, 1999.
(16) Kobayashi, M. M.Sc. Thesis, University of Toronto, Toronto, Canada, 2000.
(17) Feng, J.; Odrobina, E.; Winnik, M. A. *Macromolecules* **1998**, *31*, 5290.
(18) Kobayashi, M.; Rharbi, Y.; Winnik, M. A. *Macromolecules* **2001**, *34*, 1855.
(19) Pham, H. H.; Farinha, J. P. S.; Winnik, M. A. *Macromolecules* **2000**, *33*, 5850.
(20) Martinez, C. J.; Lewis, J. A. *Langmuir* **2002**, *18*, 4689.
(21) (a) Winnik, M. A.; Feng, J. *J. Coat. Technol.* **1996**, *68*, 39. (b) Patel, A. A.; Feng, J.; Winnik, M. A.; Vancso, J. G.; Dittman McBain, C. B. *Polymer* **1996**, *37*, 5577.
(22) (a) Guerts, J. M.; Lammers, M.; German, A. L. *Colloids Surf. A: Physicochem. Eng. Aspects* **1996**, *108*, 295. (b) Peters, A. C. I. A.; Overbeek, G. C.; Buckmann, A. J. P.; Padget, J. C.; Annable, T. *Prog. Org. Coat.* **1996**, *29*, 183.
(23) (a) Dufresne, A.; Cavaillé, J. Y.; Helbert, W. *Polym. Compos.* **1997**, *18*, 198. (b) Hajji, P.; Cavaille, J. Y.; Favier, V.; Gauthier, C.; Vigier, G. *Polym. Compos.* **1996**, *17*, 612.
(24) Tritzinou, A.; Keddie, J. L.; Guerts, J. M.; Satguru, R. *Macromolecules* **2000**, *33*, 2695.
(25) Kusy, R. P. *J. Appl. Phys.* **1977**, *48*, 5301.
(26) Eckersley, S. T.; Helmer, B. J. *J. Coat. Technol.* **1997**, *69*, 97.
(27) Wool, R. P.; O'Connor, K. M. *J. Appl. Phys.* **1981**, *52*, 5953.
(28) Keddie, J. L.; Meredith, P.; Jones, R. A. L.; Donald, A. M. *Langmuir* **1996**, *12*, 3793.
(29) Whitlow, J.; Wool, R. P. *Macromolecules* **1991**, *24*, 5926.

(30) Dhinojwala, A.; Torkelson, J. *Macromolecules* **1994**, *27*, 4817.
(31) (a) Liu, Y.; Feng, J.; Winnik, M. A. *J. Chem. Phys.* **1994**, *101*, 9096. (b) Liu, Y.; Winnik, M. A. *Macromol. Chem. Symp.* **1995**, *92*, 321.
(32) Yekta, A.; Duhamel, J.; Winnik, M. A. *Chem. Phys. Lett.* **1995**, *235*, 119.
(33) Crank, J. *The Mathematics of Diffusion*; Clarendon: Oxford, U.K., 1974.
(34) Zhao, C.-L.; Wang, Y.; Hruska, Z.; Winnik, M. A. *Macromolecules* **1990**, *23*, 4082.
(35) Farinha, J. P. S.; Martinho, J. M. G.; Yekta, A.; Winnik, M. A. *Macromolecules* **1995**, *28*, 6084.
(36) (a) Wang, Y.; Zhao, C.; Winnik, M. A. *J. Chem. Phys.* **1991**, *95*, 2143. (b) Wang, Y.; Winnik, M. A.; Haley, F. *J. Coat. Technol.* **1992**, *64*, 51. (c) Kim, H.; Wang, Y.; Winnik, M. A. *Polymer* **1994**, *35*, 1779. (d) Kim, H.; Winnik, M. A. *Macromolecules* **1994**, *27*, 1007.
(37) (a) O'Brien, J.; Cashell, E.; Wardell, G.; McBrierty, V. J. *Macromolecules* **1976**, *9*, 653. (b) Douglass, D.; McBrierty, V. J. *Polym. Eng. Sci.* **1979**, *19*, 1054. (c) Ito, M.; Nakamura, T.; Tanaka, K. *J. Appl. Polym. Sci.* **1985**, *30*, 3493. (d) Dutta, N.; Choudhury, N.; Haidar, B.; Vidal, A.; Donnet, J.; Delmotte, L.; Chezeau, J. *Polymer* **1994**, *35*, 4293. (e) Pliskin, I.; Tokita, N. *J. Appl. Polym. Sci.* **1972**, *16*, 473.
(38) (a) Tsagaropoulos, G.; Eisenberg, A. *Macromolecules* **1995**, *28*, 396. (b) Tsagaropoulos, G.; Eisenberg, A. *Macromolecules* **1995**, *28*, 6067.
(39) Wang, Y.; Winnik, M. A. *J. Phys. Chem.* **1993**, *97*, 2507.
(40) Ferry, J. D. *Viscoelastic Properties of Polymers*; Wiley: New York, 1980.
(41) Child, W. E.; Ferry, J. D. *J. Colloid Sci.* **1957**, *12*, 237. Ferry, J. D.; Strella, S. *J. Colloid Sci.* **1958**, *13*, 459.
(42) Odrobina, E. Ph.D Thesis, University of Toronto, Toronto, Canada, 2000.

MA0115951